Supporting Information

Monolithic Three-Dimensional Graphene Frameworks Derived from Inexpensive Graphite Paper as Advanced Anode for Microbial Fuel Cells

Meiqiong Chen, [†] *Yinxiang Zeng,* [†] *Yitong Zhao,* [†] *Minghao Yu,* [†] *Faliang Cheng,* [‡] *Xihong Lu,* [†,ξ,*] *and Yexiang Tong* [†*]

[†]KLGHEI of Environment and Energy Chemistry, MOE of the Key Laboratory of Bioinorganic and Synthetic Chemistry, School of Chemistry and Chemical Engineering, Sun Yat-Sen University, Guangzhou 510275, People's Republic of China
Fax: (+86)20 84112245 E-mail: luxh6@mail.sysu.edu.cn (X. H. Lu)

[‡]Biosensor Research Centre, Dongguan University of Technology, Dongguan, Guangdong, 523808, People's Republic of China.

[ξ]Jiangsu Key Laboratory of Materials and Technology for Energy Conversion, Nanjing University of Aeronautics and Astronautics, Nanjing 210016, China

Cost analysis of the 3DGFs:

Prepareing 1 m^2 3DGFs need:

Graphit paper(1 m^2) \$7.7

H_2SO_4 (7500 mL): \$24.3

HNO_3 (7500 mL): \$23.1 (the mixed acid solution can be reusable)

N_2 used in thermal reduction: \$27.9

Therefore, it takes about \$ 83 for the raw-materials to prepared 1 m^2 3DGFs (about 0.068 \$ g^{-1}).

Figures and Tables

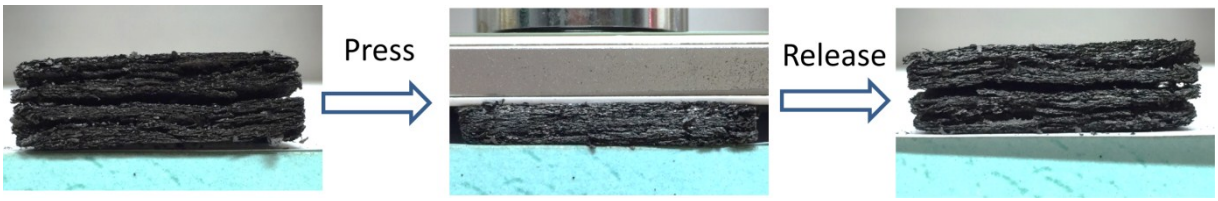

Figure S1. Digital photos of 3DGFs-30 showing the compressing and releasing process.

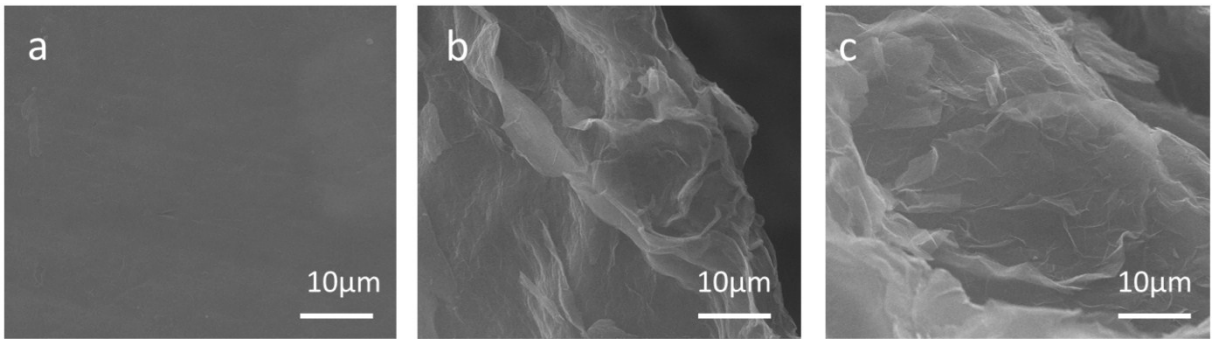

Figure S2. Low-magnification SEM images of (a) GP, (b) 3DGOFs-30, and (c) 3DGFs-30.

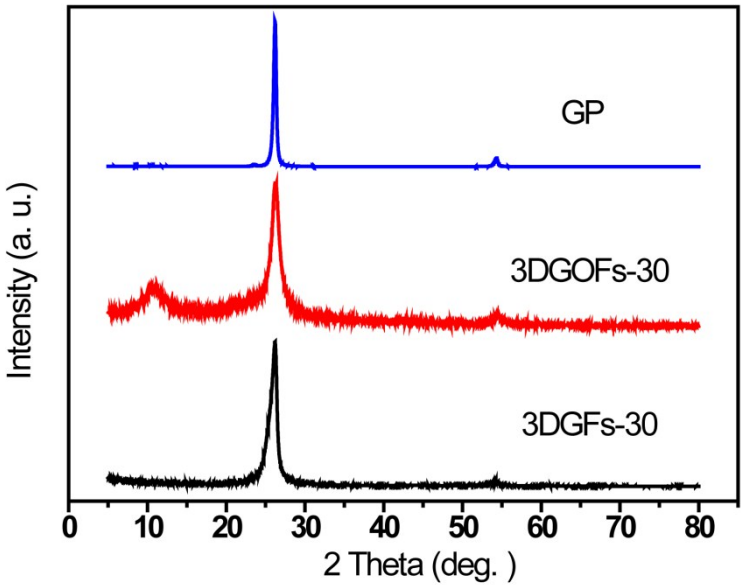

Figure S3. XRD spectra collected for GP, 3DGOFs-30, and 3DGFs-30 samples.

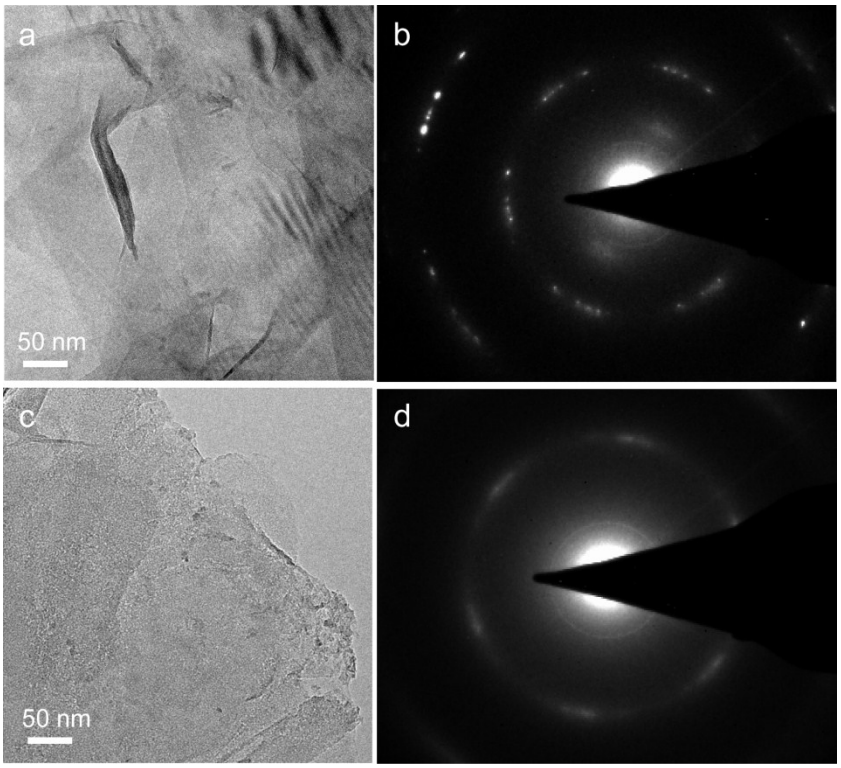

Figure S4. Low-resolution TEM image collected at the edge of (a) GP, and (c) 3DGFs-30, SAED pattern of (b) GP, and (d) 3DGFs-30.

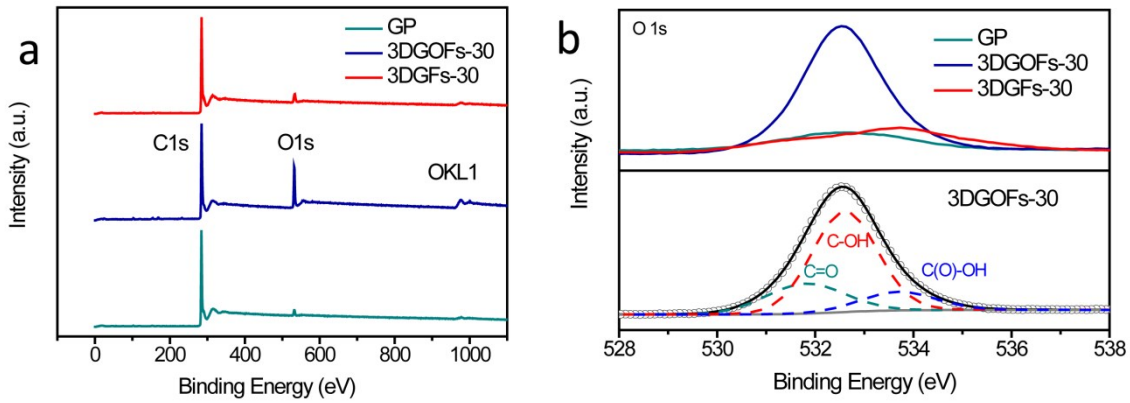

Figure S5. (a) Survey XPS spectra and (b) Upper: O 1s spectra for GP, 3DGOFs-30, and 3DGFs-30 samples, (b) Bottom: Normalized O 1s for 3DGOFs-30. The dark grey curve (scatter) is the experimental result that can be deconvoluted into three synthetic peaks (dashed lines). The black curve (solid line) is the summation of the synthetic peaks.

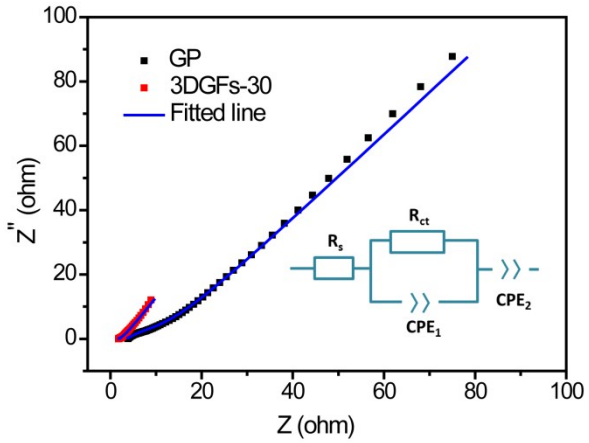

Figure S6. Nyquist plots and fitted lines of different electrodes in an anodic solution. The inset shows the equivalent circuit.

Table S1. Values of the parameters obtained from the EIS spectra of different electrodes in an anodic solution.

electrode	Rs (Ω)	Rct (Ω)	CPE_1		CPE_2	
			Yo ($Ω^{-1}$ s^n)	n	Yo ($Ω^{-1}$ s^n)	n
GP	3.52	9.37	0.02	0.46	0.05	0.58
3DGFs-30	1.18	1.20	0.49	0.42	0.47	0.67

Table S2. Summary of the performance of the previously reported 3D carbon basic anode MFCs.

Anode	Cathode	Biocatalyst	Fuel	Reactor type	MFC efficiency	References
CNT-textile	Pt loaded carbon cloth	Wastewater	Glucose	Double chamber	1098 mW m^{-2}	1
Ggraphene–sponge composite and stainless-steel current collector.	Pt loaded carbon cloth	Wastewater	Glucose	Double chamber	1.57 W m^{-2}	2
3DrGO–Ni foam	Carbon cloth	*Shewanella Oneidensis MR-1*	Trypticase soy broth	Double chamber	27 W m^{-3} (based on the volume of anode)	3
3D graphene sponge	Rectangular carbon paper	Anaerobic sludge	Acetate	Double chamber	0.71 W m^{-2}	4
3DrGO-hybrid biofilm	Carbon cloth	*Shewanella oneidensis* MR-1	Lactate	Double chamber	843 ± 31 m W m^{-2}	5
Open-celled carbon scaffold	Pt loaded carbon paper	*Escherichia coli*	Glucose	Single chamble	30.7 m W m^{-2}	6
Graphene/PANI foam	Carbon cloth	*Shewanella oneidensis* MR-1	Lactate	Double chamber	768 mW m^2	7

Reference:

1. X. Xie, L. Hu, M. Pasta, G. F. Wells, D. Kong, C. S. Criddle and Y. Cui, *Nano Lett.*, 2011, **11**, 291-296.
2. X. Xie, G. Yu, N. Liu, Z. Bao, C. S. Criddle and Y. Cui, *Energ. Environ Sci*, 2012, **5**, 6862-6866.
3. H. Wang, G. Wang, Y. Ling, F. Qian, Y. Song, X. Lu, S. Chen, Y. Tong and Y. Li, *Nanoscale*, 2013, **5**, 10283-10290.
4. W. Chen, Y.-X. Huang, D.-B. Li, H.-Q. Yu and L. Yan, *Rsc. Adv.*, 2014, **4**, 21619-21624.
5. Y.-C. Yong, Y.-Y. Yu, X. Zhang and H. Song, *Angew. Chem. Int. Ed.*, 2014, **53**, 4480-4483.
6. Y.-Q. Wang, H.-X. Huang, B. Li and W.-S. Li, *J. Mater. Chem. A.*, 2015, **3**, 5110-5118.
7. Y. C. Yong, X. C. Dong, M. B. Chan-Park, H. Song and P. Chen, *ACS nano*, 2012, **6**, 2394-2400.

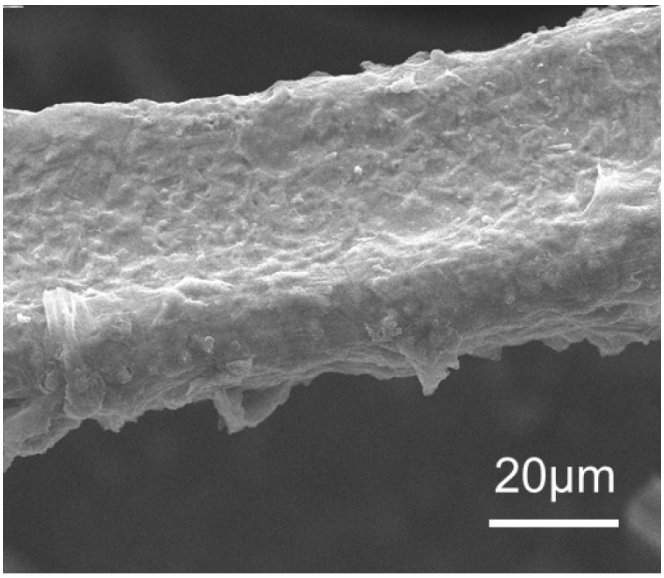

Figure S7. SEM images of 3D reduced graphene oxide/Ni foam (3DRGO/Ni).

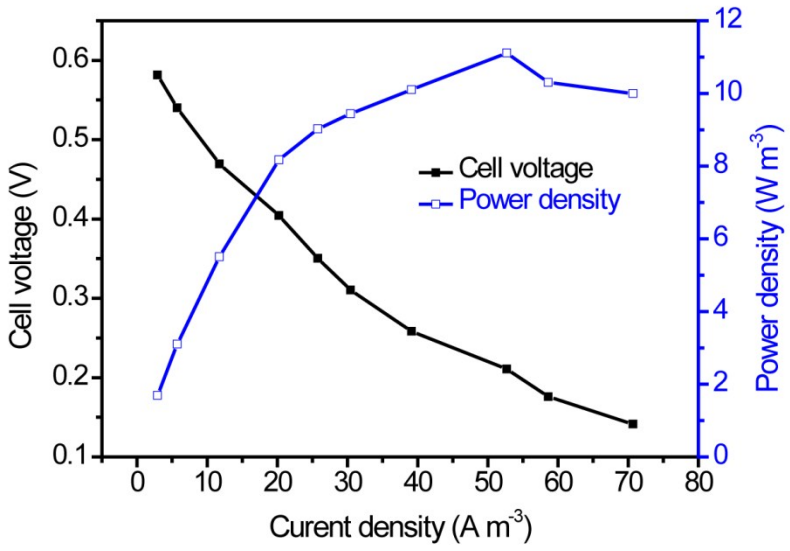

Figure S8. Power output and polarization curve of 3DRGO/Ni-MFC and 3DGFs-MFC.

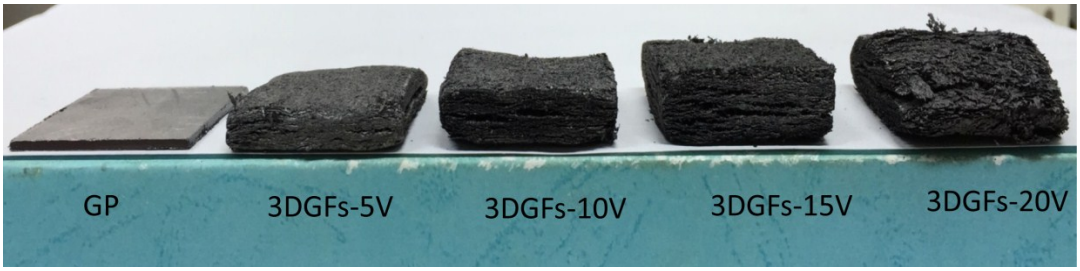

Figure S9. Comparison of the digital images of GP, and 3DGFs oxidation with 30 minutes at different potential.

The relationships between the performance and the oxidation potential of 3DGFs as well as oxidation time were also studied. As shown in Figure S7, the volume of 3DGFs electrode increased obviously with the increase of oxidation potential from 5 to 20 V. Simultaneously, the 3DGFs electrdoes obtained at the higher potential possessed faster mass diffusion rate, which is confirmed by the more steeper straight lines of their Nyquist plots (Figure S8). However, structural collapsing was observed for the 3DGFs electrode obtained at 20 V (Figure S7), which lead to the decrease of the output power (Figure S9). Therefore, the oxidation potential was set at 15 V to study the effect of oxidation time on the performance of the 3DGFs. As shown in Figure S10 and Figure S11, the BET surface area and pore volume of 3DGFs electrode increased with the increase of oxidation time from 10 to 30 min and then decreased over 30 min. In addition, the CV (Figure S13) and EIS (Figure S14) tests confirmed that the 3DGFs-30 electrode possessed best electrocatalytic activity and lowest charge-transfer resistance than other 3DGFs electrodes obtained at different time. Therefore, the MFC based on 3DGFs electrode obtained at a potential of 15 V for 30 min has the best performance (Figure S15 and S16).

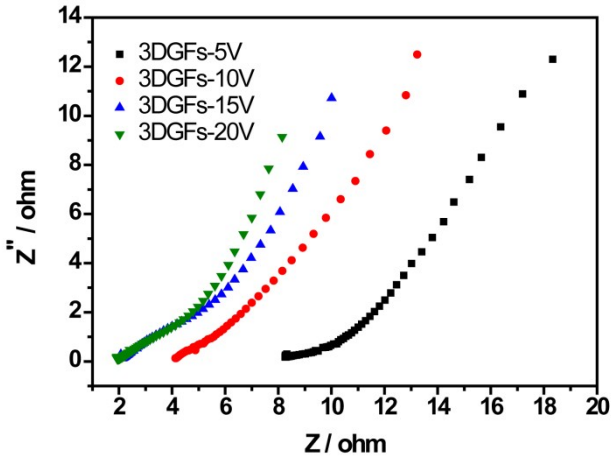

Figure S10. Nyquist plots of different 3DGFs anode (oxidation with 30 minutes at different potential) in an anodic solution.

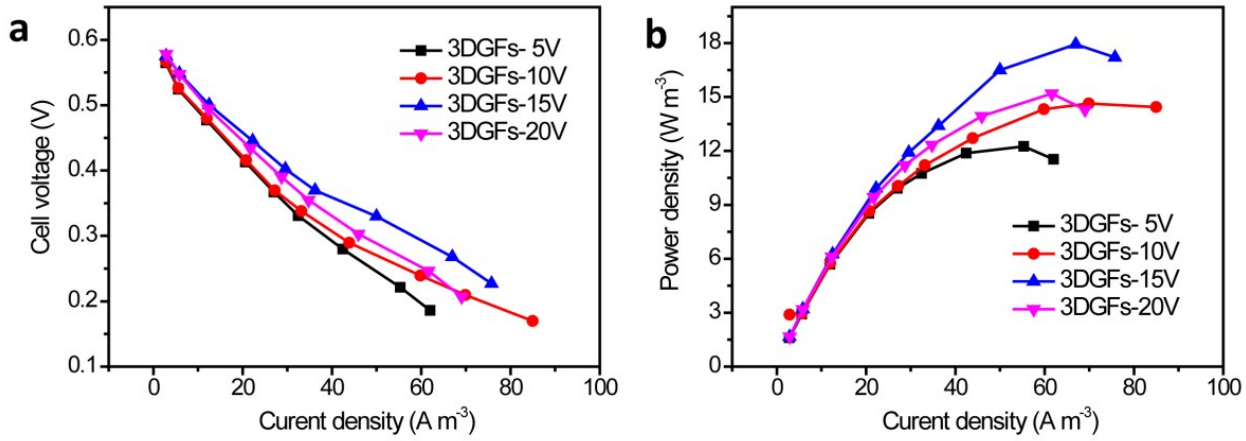

Figure S11. (a) Power output, and (b) polarization curve of MFC with different 3DGFs anode (oxidation with 30 minutes at different potential).

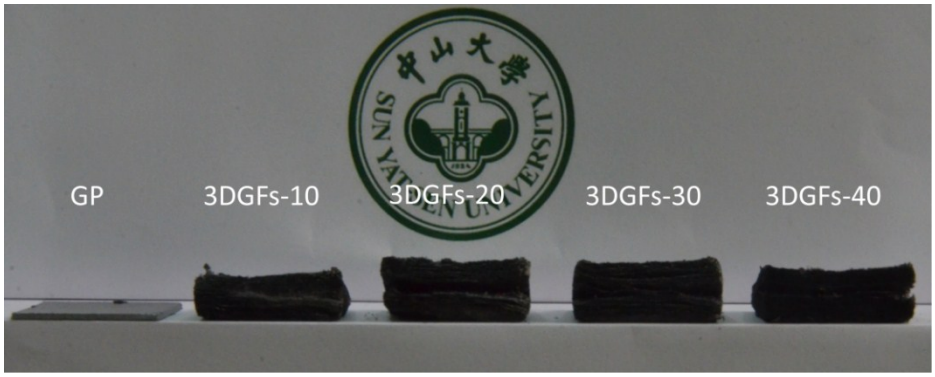

Figure S12. Comparison of the digital images of GP and 3DGFs obtained with oxidation time of 10minutes (3DGFs-10), 20minutes (3DGFs-20), 30minutes (3DGFs-30) and 40minutes (3DGFs-40).

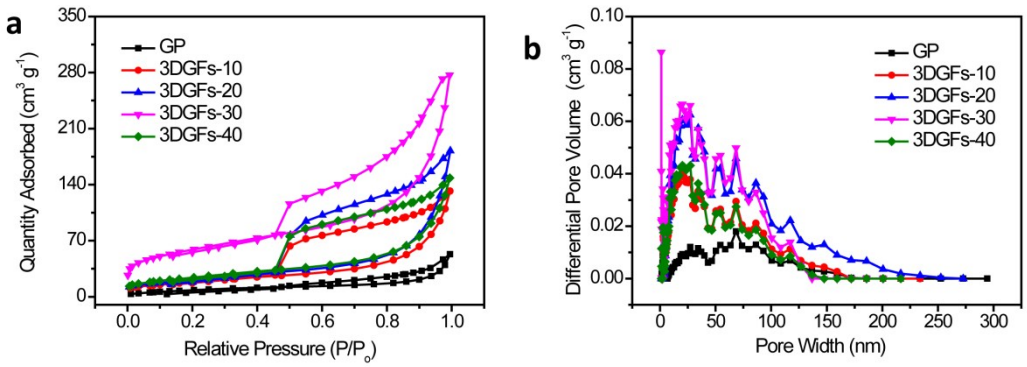

Figure S13. (a) Nitrogen adsorption isotherms and (b) Pore-width and pore-volume distribution of GP, 3DGFs-10, 3DGFs-20, 3DGFs-30 and 3DGFs-40 at 77 K.

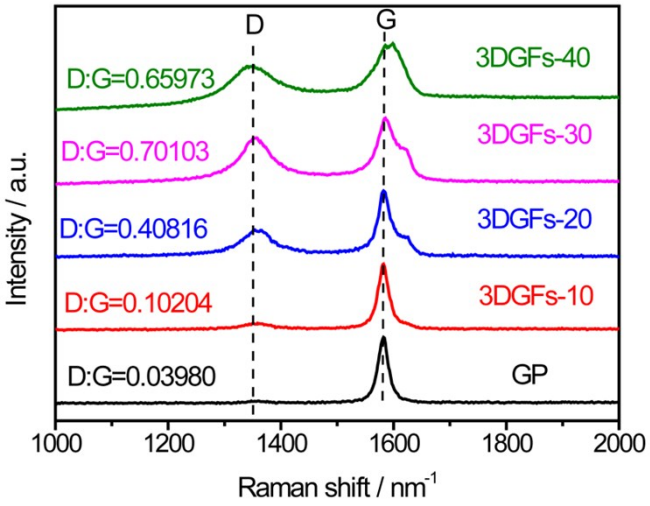

Figure S14. Raman spectra of GP, 3DGFs-10, 3DGFs-20, 3DGFs-30 and 3DGFs-40.

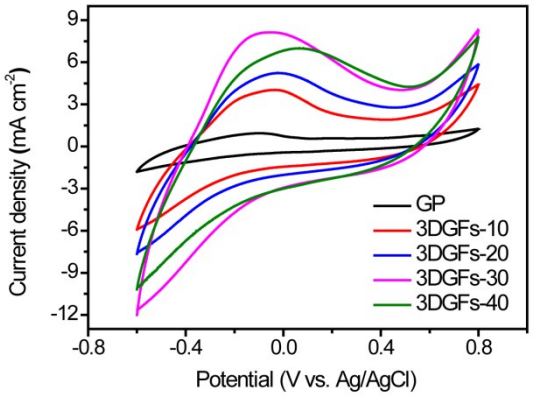

Figure S15. Cyclic votammograms of different electrode, collected in anodic solution (with glucose), at a scan rate of 10 mV s^{-1}

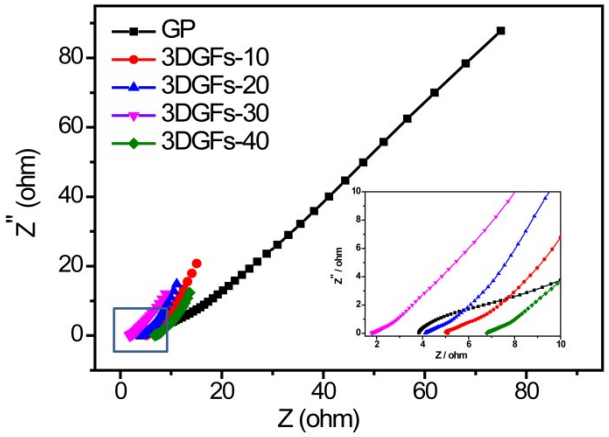

Figure S16. Nyquist plots of different electrodes in an anodic solution. The inset illustrates the high-frequency part of the result.

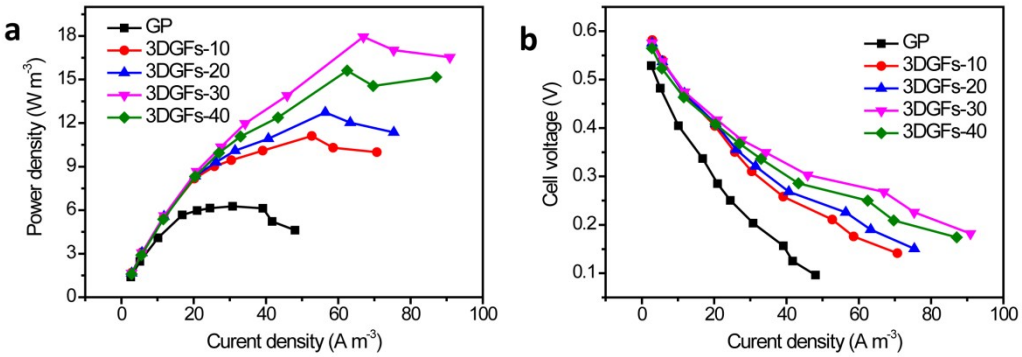

Figure S17. (a) Power outputs, and (b) polarization curves of MFC with different anode.

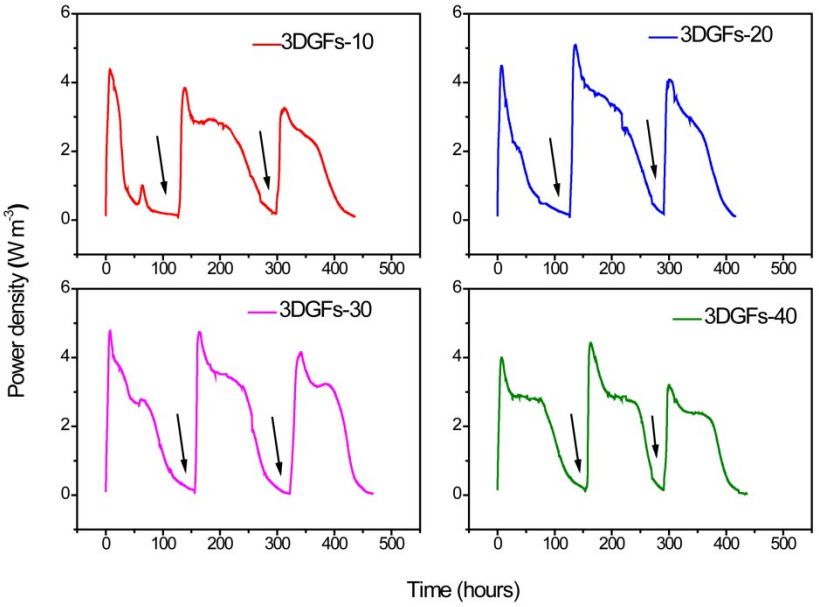

Figure S18. Power generation of different anode MFC operated in a batch-fed mode with a 1 kΩ loading. Arrows indicate replacement of the glucose medium. The volumetric power densities were calculated based on the volume of the anode chamber (~20mL)

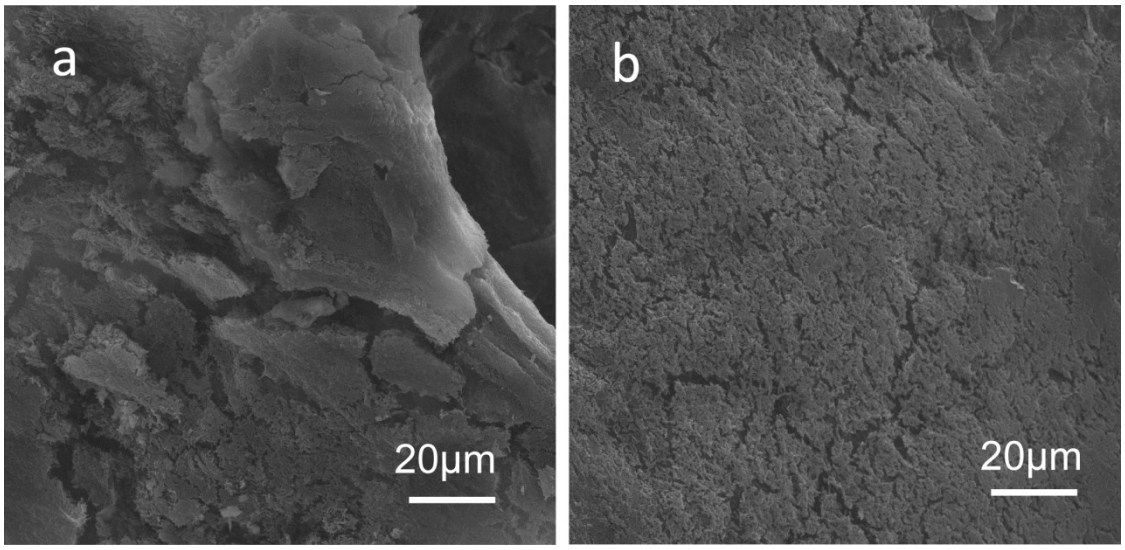

Figure S19. Low-magnification SEM images of colonized (a) 3DGFs-30, and (b) GP anode obtained after three consecutive feeding cycles of MFC.

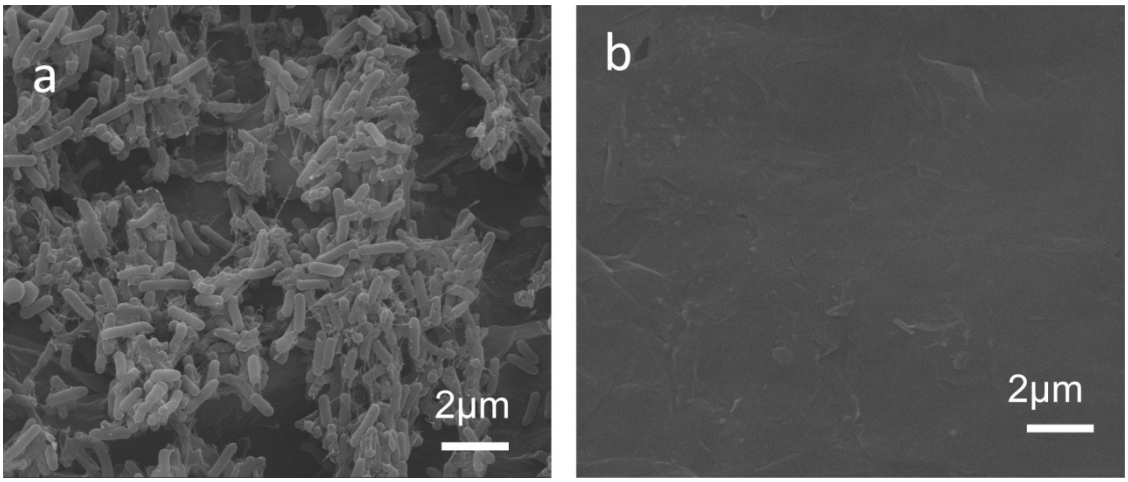

Figure S20. SEM images of colonized GP anode, obtained after three consecutive feeding cycles of MFC, (a) exterior and (b) inside.